CrystEngComm

Accepted Manuscript

ROYAL SOCIETY OF CHEMISTRY

www.rsc.org/crystengcomm

Manuscript ID CE-ART-01-2014-000215.R1

Preparation, crystal structures and conformation of six complexes based on 1,4-bis(benzimidazol-1-ylmethyl)-2,3,5,6-tetramethylbenzene

Qing-Xiang Liu*, Zhi-Xiang Zhao, Xiao-Jun Zhao, Yue Bi, Jie Yu and Xiu-Guang Wang

Tianjin Key Laboratory of Structure and Performance for Functional Molecules; Key Laboratory of Inorganic-Organic Hybrid Functional Material Chemistry, Ministry of Education; College of Chemistry, Tianjin Normal University, Tianjin 300387, China.
* Corresponding author, E-mail: tjnulqx@163.com

Reaction of ligands (**L** or $\mathbf{L_A}$) with metal salts affords six new metal complexes $\{[Mn(L)_3](ClO_4)_2\}_n$ (**1**), $[Cu(L)(SO_4)(H_2O)]\cdot 1.5H_2O$ (**2**), $[Co(L)(L_A)(CH_3OH)_2]\cdot 2CH_3OH$ (**3**), $[Co(L)(DMF)(NO_3)_2]_n$ (**4**), $[Cd(L)(DMF)(NO_3)_2]_n$ (**5**) and $[Cu(L)(DMF)(NO_3)_2]_n$ (**6**) (**L** = 1,4-bis(benzimidazol-1-ylmethyl)-2,3,5,6-tetramethylbenzene, $\mathbf{L_A}$ = fumarate). These complexes are structurally characterized by X-ray diffraction analyses. Analyses of crystal structures of complexes **1** and **2** show that 2D layers with metallomacrocycles are formed via ligand **L** and metal atoms (Mn(II) for **1** and Cu(II) for **2**). 2D layer with metallomacrocycles in complex **3** is formed via ligand **L**, fumarate groups and Co(II) atoms. 1D polymeric chains in complexes **4**-**6** are formed via ligand **L** and metal atoms (Co(II) for **4**, Cd(II) for **5** and Cu(II) for **6**). In the crystal packings of complexes **1**-**6**, 3D supramolecular frameworks are formed via intermolecular weak interactions, including π-π interactions and C-H···π contacts. π-π interactions between benzimidazole rings are compared. The conformations of metal complexes based on dibenzimidazolyl bidentate ligands with flexible or semi-rigid linkers are described and compared. Additionally, the fluorescence emission spectra of ligand **L** and metal complexes, and the magnetic properties for complexes **2**-**4** are reported.

Keywords: Manganese(II); Copper(II); Cobalt(II); Cadmium(II); Complexes; Dibenzimidazolyl Ligand

Introduction

Construction of metal-organic frameworks (MOFs) and porous coordination polymers have drawn much attention due to their promising applications in molecular recognition, ion exchange, chemical sensors, catalysis and separation.[1] So far, a large number of metal-organic frameworks with different structures have been synthesized by purposeful design and use of particular ligands, such as grids, honeycombs and diamondoid nets with rigid ligands,[2] and helixes and crossing structures with flexible ligands.[3] During the course of preparation of complexes, the choice of ligand is of vital importance. The use of rigid ligands may lead to some controllable structures of MOFs,[2a,4] and the use of flexible bridging ligands will lead to less predictable structures.[5] Among the organic ligands, the ligands containing benzimidazole (or imidazole) rings play important roles in coordination chemistry, and they can coordinate with a variety of transition metals to form one-, two- and three-dimentional coordination compounds through using nitrogen atoms of benzimidazole (or imidazole).[6] The benzimidazole ring is a structural component of many compounds occurring in living organisms.[7] Hence, the investigating structures of metal complexes from benzimidazole has significance toward understanding the coordinating process between the benzimidazole rings and metal ions in life science.

One of the most effective strategies to assemble MOFs is to apply multifunctional organic ligands to connect metal atoms.[8] We are interested in the dibenzimidazolyl bidentate ligands with different linkers. Our group has reported the coordination chemistry of some diimidazolyl (or dibenzimidazolyl) ligands bearing flexible linkers (such as oligoether linkers and alkanyl linkers).[9] In order to understand further the differences of structures of metal complexes based on dibenzimidazolyl bidentate ligands with flexible or semi-rigid linkers, we here report a series of new metal complexes based on dibenzimidazolyl bidentate ligand with semi-rigid 2,3,5,6-tetramethylbenzene linker. These new metal complexes include $\{[Mn(L)_3](ClO_4)_2\}_n$ (**1**), $[Cu(L)(SO_4)(H_2O)]\cdot 1.5H_2O$ (**2**), $[Co(L)(L_A)(CH_3OH)_2]\cdot 2CH_3OH$ (**3**), $[Co(L)(DMF)(NO_3)_2]_n$ (**4**), $[Cd(L)(DMF)(NO_3)_2]_n$ (**5**) and $[Cu(L)(DMF)(NO_3)_2]_n$ (**6**) (**L** = 1,4-bis(benzimidazol-1-ylmethyl)-2,3,5,6-tetramethylbenzene, $\mathbf{L_A}$ = fumarate). Additionally, π-π interactions between benzimidazole rings are compared. The conformations of metal complexes based on dibenzimidazolyl bidentate ligands with flexible or semi-rigid linkers are described and compared. At the same time, the

fluorescence emission spectra of ligand **L** and metal complexes **1-6**, and the magnetic properties for complexes **2-4** are reported.

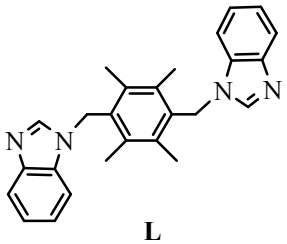

L

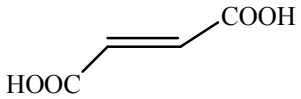

H_2L_A

Results and discussion

Synthesis and characterization of ligand L and metal complexes 1-6

1,4-Bis(bromomethyl)-2,3,5,6-tetramethylbenzene was prepared via the reaction of 1,2,4,5-tetramethylbenzene with paraformaldehyde and HBr. The ligand 1,4-bis(benzimidazol-1-ylmethyl)-2,3,5,6-tetramethylbenzene (**L**) was prepared through the reaction of benzimidazole with 1,4-bis(bromomethyl)-2,3,5,6-tetramethylbenzene (Scheme 1). The ligand **L** is soluble in common organic solvents (such as CH_3OH, DMF and DMSO), therefore, the crystallization of its complexes with inorganic metal salts occurs readily.

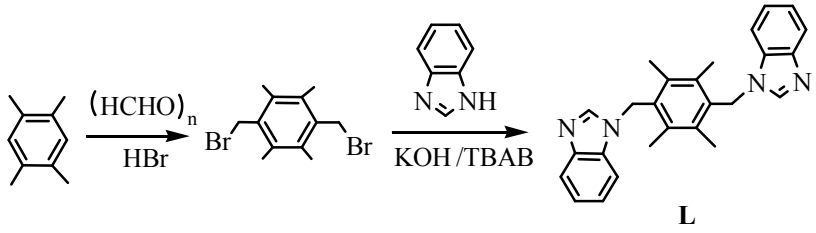

L

Scheme 1 Preparation of ligand **L**

Complexes $\{[Mn(L)_3](ClO_4)_2\}_n$ (**1**), $[Cu(L)(SO_4)(H_2O)]\cdot 1.5H_2O$ (**2**), $[Co(L)(DMF)(NO_3)_2]_n$ (**4**), $[Cd(L)(DMF)(NO_3)_2]_n$ (**5**) and $[Cu(L)(DMF)(NO_3)_2]_n$ (**6**) were prepared via the reaction of ligand **L** with metal salts ($Mn(ClO_4)_2\cdot 6H_2O$ for **1**, $CuSO_4\cdot 5H_2O$ for **2**, $Co(NO_3)_2\cdot 6H_2O$ for **4**, $Cd(NO_3)_2\cdot 4H_2O$ for **5** and $Cu(NO_3)_2\cdot 3H_2O$ for **6**) in DMF/CH_3OH. Complex $[Co(L)(L_A)(CH_3OH)_2]\cdot 2CH_3OH$ (**3**) was prepared via the reaction of **L** and fumaric acid with $Co(NO_3)_2\cdot 6H_2O$ in the presence of Et_3N in DMF/CH_3OH. The crystals of **1-6** suitable for X-ray diffraction were grown by

evaporating slowly their DMF/CH_3OH solution at room temperature. Complexes **1-6** are stable and can retain their structural integrity at room temperature for a considerable length of time.

Structures of complexes 1-4

In the complexes **1-4** (Fig. 1(a)-Fig. 4(a)), the dibenzimidazolyl bidentate ligand **L** adopt trans-conformation (namely, two benzimidazole rings lie in the two sides of 2,3,5,6-tetramethylbenzene plane) as shown in Scheme 1. In each ligand of complexes, two benzimidazole rings are parallel (complexes **1**, **3** and **4)** or nearly parallel (complex **2**), and the dihedral angles between the 2,3,5,6-tetramethylbenzene and two benimidazole rings are 81.5-89.7° (Table 1). The differences of these dihedral angles may originate in the different metal center connected to ligand and different coordination environment around metal center.

Table 1 The dihedral angles between two benzimidazole rings (A), and between the 2,3,5,6-tetramethylbenzene and two benimidazole rings (B) in each ligand

Complexes	A (°)	B (°)
1	0	85.5
2	4.9	83.2, 87.3
3	0	89.7
4	0	81.5

In complex **1** (Fig. 1(a)), 2D network layer with 39-membered rotiform metallomacrocycles is formed by ligand **L** and Mn(II) atom, in which each rotiform metallomacrocycle is constructed by three bidentate ligands **L** and three Mn(II) atoms (Fig.1(b)). In each metallomacrocycle, two adjacent 2,3,5,6-tetramethylbenzene planes form the dihedral angles of 61.0(1)°, 67.0(5)° and 67.3(3)°; three Mn(II) atoms form an equilateral triangle, where the neighboring Mn···Mn separations are 13.468(8) Å. Each Mn(II) atom is surrounded by six nitrogen atoms from six benzimidazole rings to afford a slightly distorted octahedral geometry. Among six benzimidazole rings connected to Mn(II) center, the adjacent two benzimidazole rings form the same dihedral angle of 86.6(0)°, and three pairs of benzimidazole rings located in the opposite sides are parallel to each other, respectively. The bond distances of six Mn-N are all 2.280(2) Å, which are

fall in the reported ranges of 1.974(2)-2.521(3) Å.[10] The three bond angles of N(1)-Mn(1)-N(1C), N(1A)-Mn(1)-N(1D) and N(1B)-Mn(1)-N(1E) are all 180.0(1)˚, and the bond angles of other N-Mn-N range from 85.6(9)˚ to 94.3(1)˚.

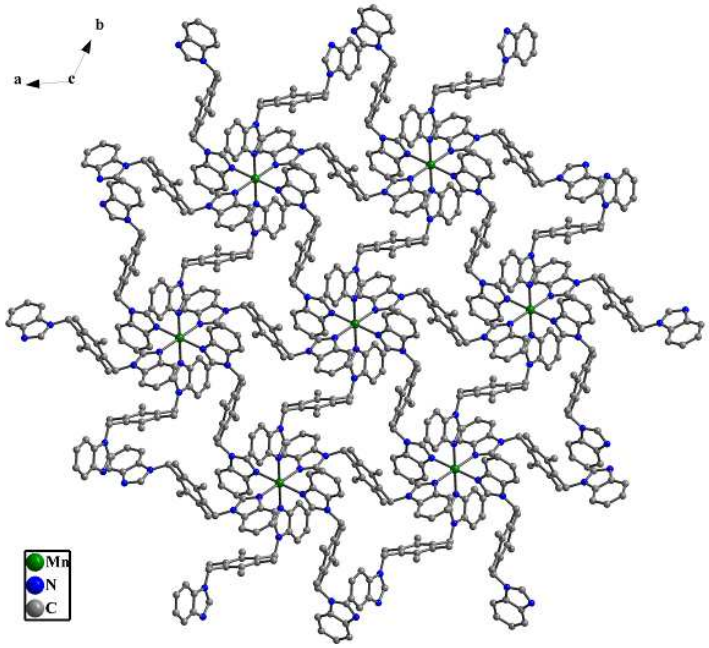

(a)

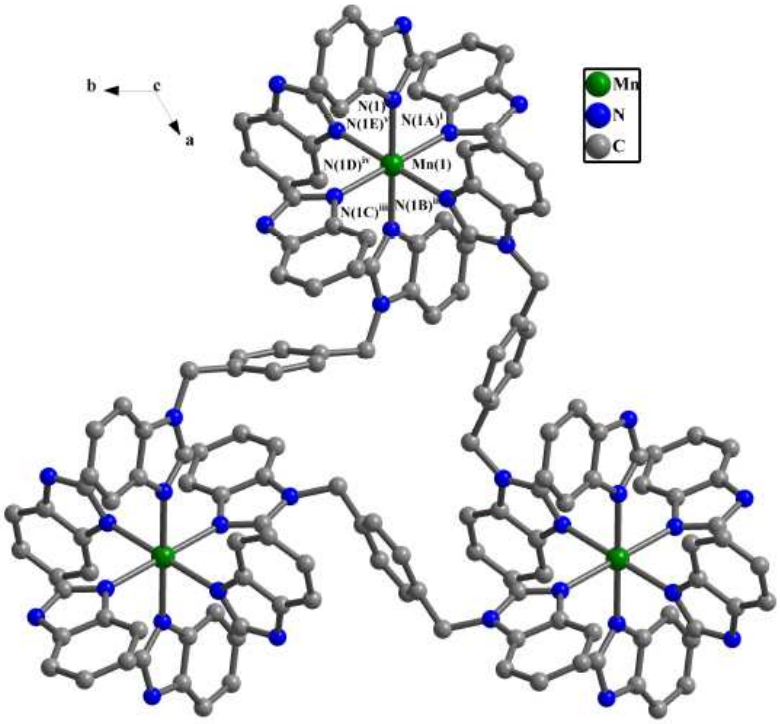

(b)

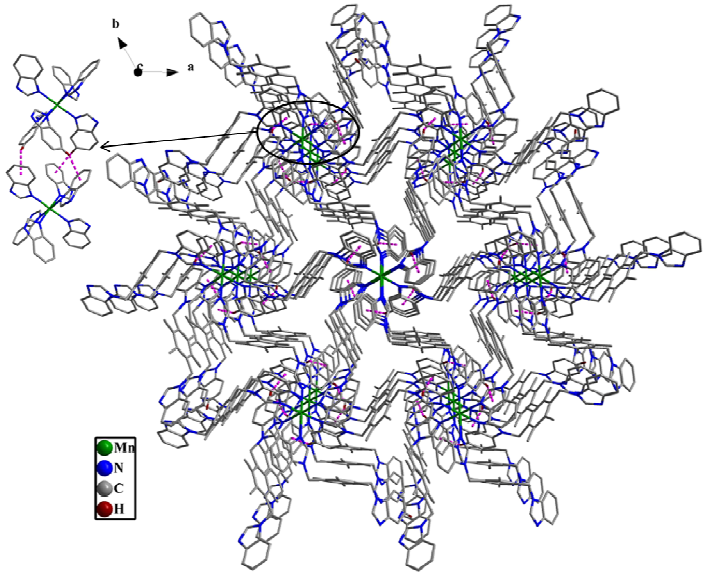

(c)

Fig. 1 (a) 2D layer of complex **1**. All hydrogen atoms were omitted for clarity. (b) A view of rotiform metallomacrocycle for **1** and all methyl groups were omitted for clarity. Symmetry code: i = *x* - *y*, *x*, 1- *z*; ii = -*y*, *x* - *y*, *z*; iii = -*x*, -*y*, 1 - *z*; iv = -*x* + *y*, -*x*, *z*; v = *y*, -*x* + *y*, 1 - *z*. (c) 3D supramolecular frameworks of complex **1** via C-H···π contacts. All hydrogen atoms except those participating in the C-H···π contacts were omitted for clarity.

Analysis of the crystal structure of **2** shows that 2D network layer with 60-membered metallomacrocycles is formed via ligands **L**, Cu(II) atoms and SO_4^{2-} (Fig. 2(a)). Each metallomacrocycle is constructed by four ligands **L**, six Cu(II) atoms and four sulfate groups, in which the cross two pairs of 2,3,5,6-tetramethylbenzenes are parallel to each other, respectively, and adjacent two 2,3,5,6-tetramethylbenzenes form the dihedral angle of 70.6(8)˚. Two sulfate groups and two Cu(II) atoms form a 8-membered ring as a part of 60-membered metallomacrocycle. Two benzimidazole rings connected to the same Cu(II) atom are approximately perpendicular with the dihedral angles of 84.6(3)˚. Each Cu(II) atom is penta-coordinated with two nitrogen atoms from two benzimidazole rings of two ligands **L**, and three oxygen atoms (two oxygen atoms being from two sulfate groups and the third oxygen atom being from one water molecule) to adopt a trigonal bipyramid geometry. The axial position of trigonal bipyramid is occupied by N(1) and

O(6) with axial distances of 1.956(3) Å and 1.958(3) Å, and the N(1)-Cu(1)-O(6) angle of 170.8(0)˚. Three N(4A), O(1) and O(2A) atoms lie in the equatorial plane. The bond distance of Cu(1)-N(1) is 1.956(3) Å, which is slightly shorter than the known values of 1.990(3) Å-2.237(2) Å.[11] The bond distance of Cu(1)-O(1) is 1.951(3) Å, which is fall in normal ranges of 1.930(6) Å-1.951(9) Å.[11] The bond distance of Cu(1)-O(2) is 2.490(9) Å, which is slightly longer than known values.

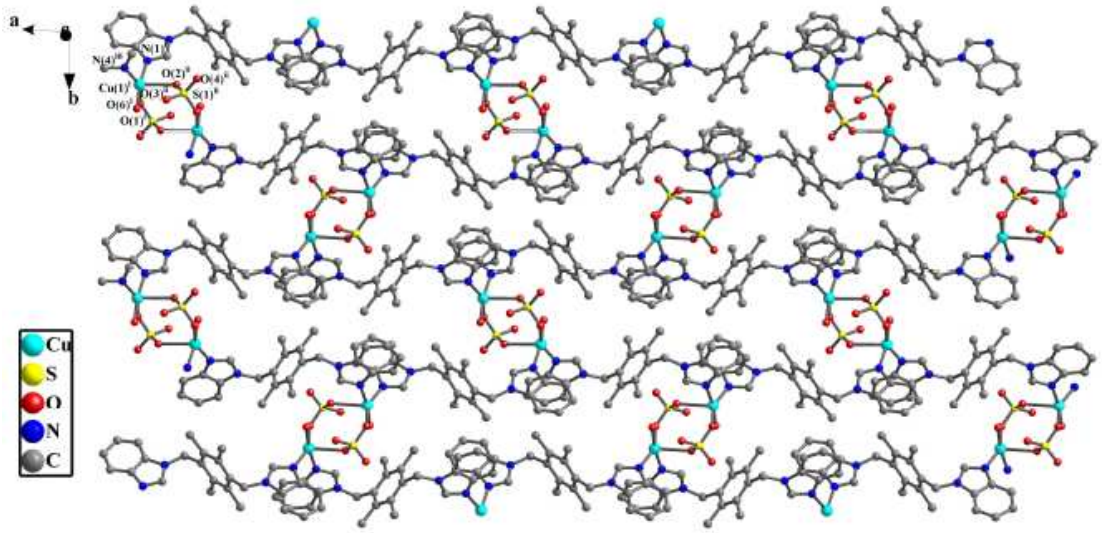

(a)

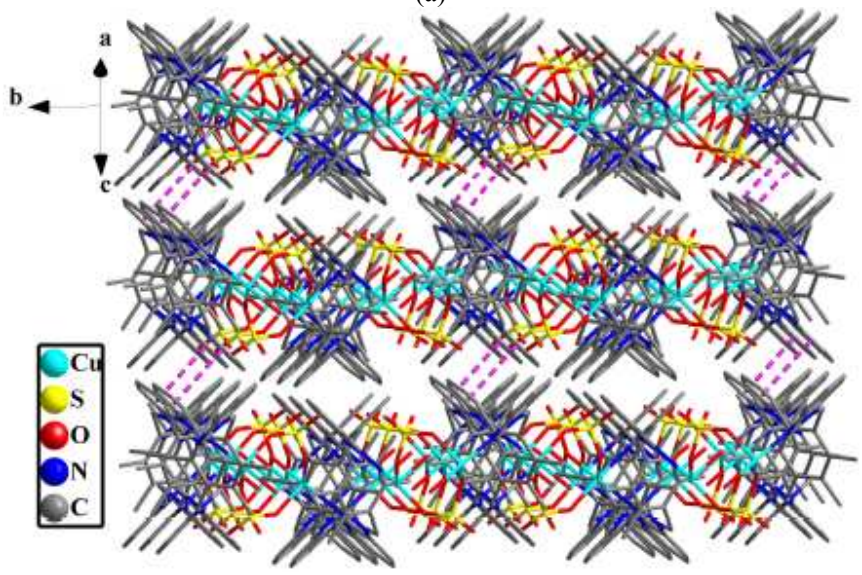

(b)

Fig. 2 (a) 2D layer of complex **2**. All hydrogen atoms were omitted for clarity. Symmetry code: i = 2 + *x*, -1 + *y*, 1 + *z*; ii = 3 - *x*, -*y*, 2 - *z*; iii = 3 + *x*, -0.5 - *y*, 1.5 + *z*. (b) 3D supramolecular frameworks of complex **2** via π-π interactions. All hydrogen atoms were omitted for clarity.

In the crystal structure of **3** (Fig. 3(a)), an interesting feature is that 2D network layer with 44-membered metallomacrocycles is formed by ligands **L**, fumarate groups and Co(II) atoms, in which each metallomacrocycle is constructed by two bidentate ligands **L**, two fumarate groups and four Co(II) atoms. In each metallomacrocycle, two 2,3,5,6-tetramethylbenzenes are parallel to each other, the Co···Co separation in two sides of fumarate group is 9.144(4) Å, and the Co···Co separation in two sides of bidentate ligand is 12.463(7) Å. Two benzimidazole rings connected to the same Co(II) is parallel. Each Co(II) atom is surrounded by two nitrogen atoms from two benzimidazole rings of two ligands **L** and four oxygen atoms (two oxygen atoms being from two carboxyl groups of two fumarates, and other two oxygen atoms being from two CH_3OH molecules) to adopt a slightly distorted octahedral geometry. In the octahedron, the bond distances of Co(1)-N(1) and Co(1)-N(1A) are the same (2.083(3) Å), which are fall in the normal ranges of 2.005(6) Å-2.200(4) Å.[12] The bond distances of Co(1)-O(1) and Co(1)-O(3) are 2.077(3) Å and 2.142(3) Å, respectively, and these values are fall in the normal ranges of 1.950(8) Å-2.367(3) Å.[12] The bond angles of N(1)-Co(1)-N(1A), O(1)-Co(1)-O(1A) and O(3)-Co(1)-O(3A) are all 180.0(0)°. The bond angles of O(1)-Co(1)-O(3) and O(1)-Co(1)-O(3A) are 88.5(9)° and 91.4 (1)°, respectively. The bond angles of N-Co-O range from 86.7(4)° to 93.2(6)°. These values are fall in the normal ranges of 86.4(3)°-140.3(3)°.[12]

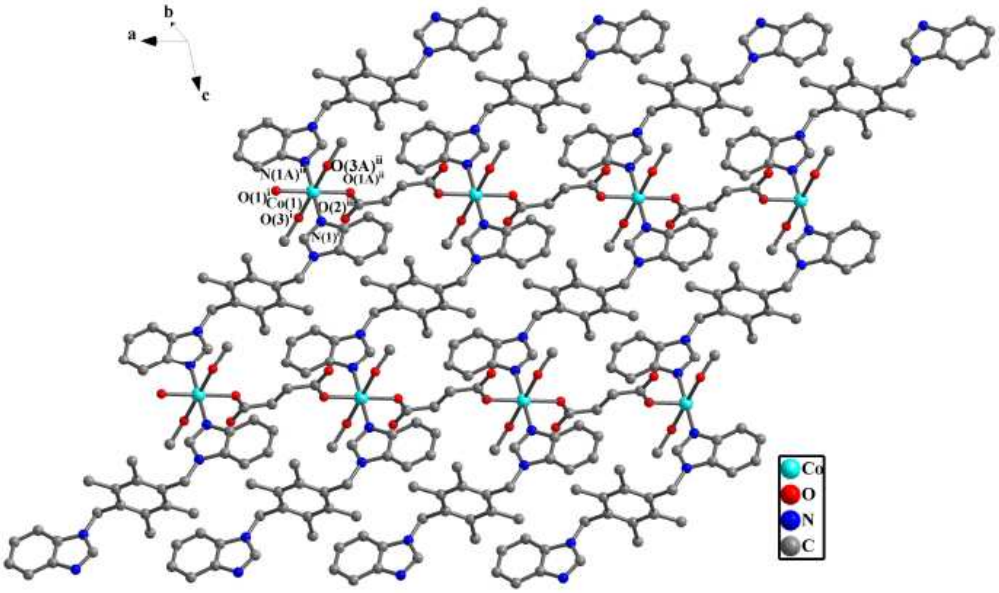

(a)

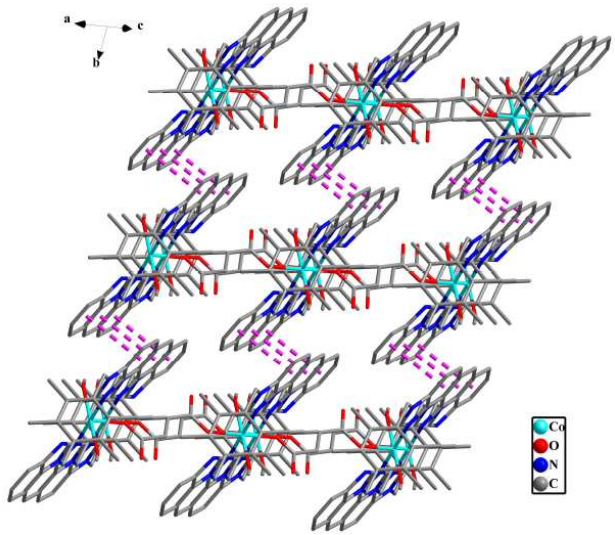

(b)

Fig. 3 (a) 2D layer of complex **3**. All hydrogen atoms were omitted for clarity. Symmetry code: i = 2 + *x*, *y*, *z*; ii = 3 - *x*, 1 - *y*, -*z*. (b) 3D supramolecular frameworks of complex **3** via π-π interactions. All hydrogen atoms were omitted for clarity.

1D polymeric chains of complex **4** was formed via ligand **L** and Co(II) atoms as shown in Fig. 4(a). The dihedral angles between two benzimidazole rings connected to the same metal atom are 78.4(1)˚. In 1D polymeric chain, all interval 2,3,5,6-tetramethylbenzenes are parallel to each other, respectively, and adjacent two 2,3,5,6-tetramethylbenzenes form the dihedral angles of 20.9(3)˚. Each metal center is seven-coordinated with two nitrogen atoms from two benzimidazole rings of two ligands **L** and five oxygen atoms (four oxygen atoms being from two nitrate groups and the fifth oxygen atom being from one DMF molecule) to adopt pentagonal bipyromidal coordination polyhedron. The axial positions of pentagonal pyramid are occupied by N(1) and N(1A) with N(1)-Co(1)-N(1A) bond angles of 174.5(2)˚. The bond distances of Co(1)-N(1), Co(1)-O(1), Co(1)-O(2) and Co(1)-O(4) are 2.101(4) Å, 2.231(5) Å, 2.205(4) Å and 2.118(6) Å, respectively. The bond angles of N(1)-Co(1)-O(2), N(1)-Co(1)-O(4) and O(2)-Co(1)-O(4) are 98.1(8)˚, 93.1(4)˚ and 148.6(2)˚, respectively. These values are similar to those of complex **3** and known Co(II) complexes.[12]

Complexes **5** and **6** (Fig. S1(a) and Fig. S2(a) in Supplementary Information)

contain similar 1D polymeric chains compared with complex **4**, and only their metal atoms are different from **4** (Cd(II) for **5** and Cu(II) for **6**). The crystal structure discussion and the crystal packings of **5** and **6** are given in Supplementary Information.

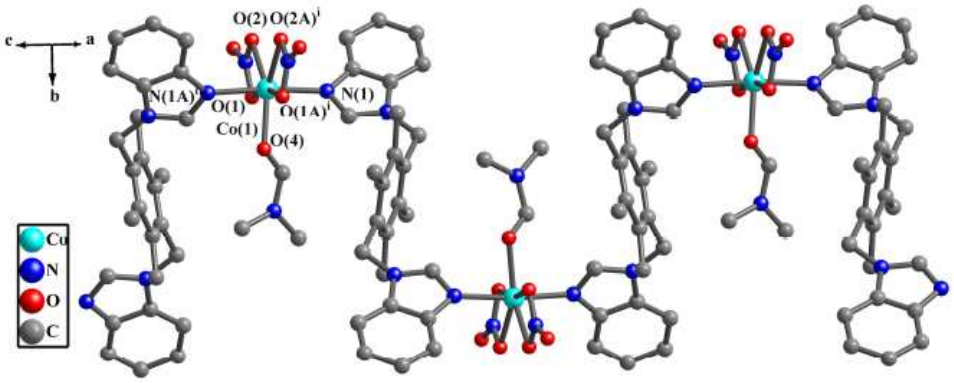

(a)

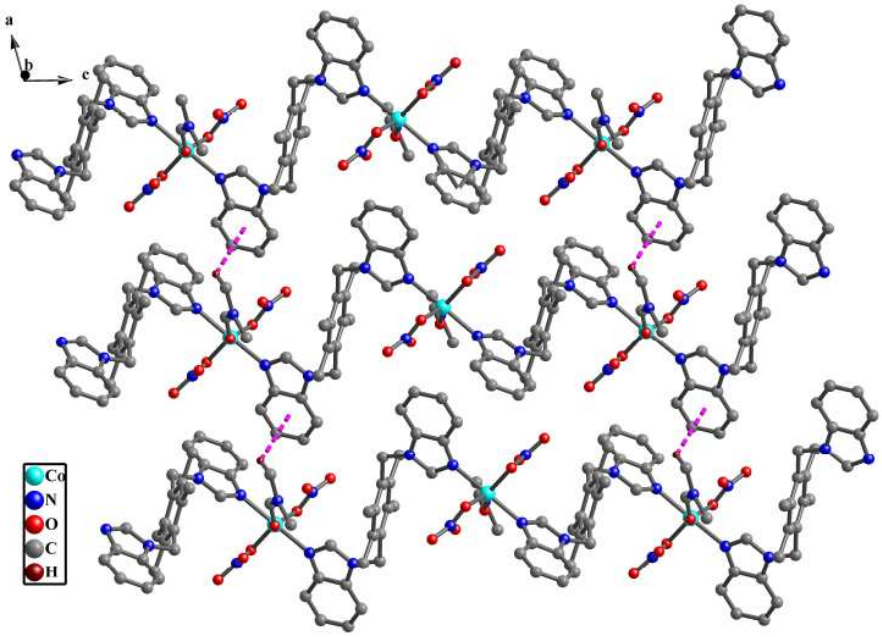

(b)

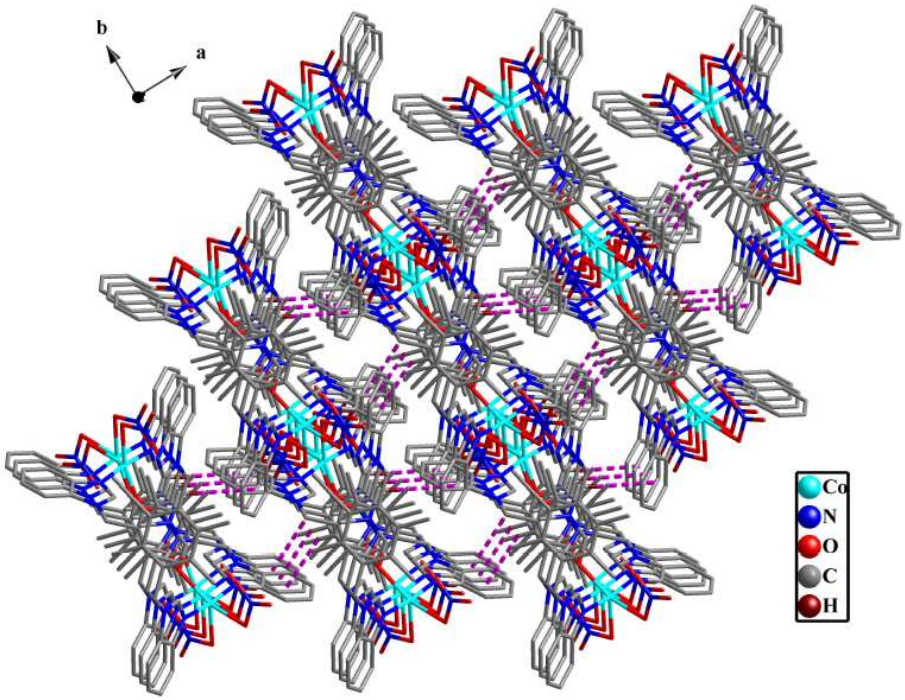

(c)

Fig. 4 (a) 1D polymeric chain of complex **4**. All hydrogen atoms were omitted for clarity. Symmetry code: i = -*x*, *y*, 0.5 - *z*. (b) 2D supramolecular layer of complex **4** via C-H···π contacts. All hydrogen atoms except those participating in the C-H···π contacts were omitted for clarity. (c) 3D supramolecular network of complex **4** via C-H···π contacts. All hydrogen atoms except those participating in the C-H···π contacts were omitted for clarity.

The crystal packings of complexes 1-4

In the crystal packing of **1** (Fig. 1(c)), 2D layers are linked together via interlayer C-H···π contacts to form 3D supramolecular frameworks. In C-H···π contacts, the hydrogen atoms are from benzimidazole rings and π systems are from benzimidazole rings. The description on C-H···π contacts has been reported,[13] and the values of C-H···π contacts are fall in the normal range as shown in Table S1.

In the crystal packings of **2** and **3** (Fig. 2(b) and Fig. 3(b)), 2D layers are assembled into 3D supramolecular architectures via π-π interactions from intermolecular benzimidazole rings. π-π interactions play important roles in self-assembly or molecular recognition processes, and they along with other weak interactions (such as hydrogen

bonds and C-H···π contacts) can provide more opportunities for constructing supramolecular architectures.[14] Benzimidazole is a dipole molecule due to the electron-withdrawing effect of nitrogen atoms, in which the benzene ring is electron deficient moiety, and the imidazole ring is electron rich moiety. When the nitrogen atom of benzimidazole coordinates with a metal atom, the electron-withdrawing effect of the metal atom with positive charge further enhances the polarity of benzimidazole. Therefore, the benzimidazole rings in the metal complexes engage easily in π-π stacking interactions between molecules.

According to literature reports, the order of stability in the interactions of two π systems is: π-deficient···π-deficient > π-deficient···π-rich > π-rich···π-rich.[15] π-π interactions between two benzimidazole rings include mainly tail-to-tail type (I), head-to-tail type (II) and head-to-head type (III) (Scheme 2), in which the tail-to-tail type belongs to π-deficient···π-deficient, the head-to-tail type belongs to π-deficient···π-rich, and the head-to-head type belongs to π-deficient···π-deficient in the end of benzene and to π-rich···π-rich in the end of imidazole. In this case, the two benzimidazole rings are easily not parallel due to the difference of acting force in two ends to lead to weak π-π interactions. Therefore, the order of stability in π-π interactions of two benzimidazole rings is: tail-to-tail > head-to-tail > head-to-head. Experimental results also show that the tail-to-tail type (such as complexes **2** and **3**, and known complexes[16]) and head-to-tail type[17] are common cases. Whereas, the head-to-head type is a rare phenomenon, and only a few metal complexes with special structures can adopt this type (like {Ag_2[bis(2-benzimidazol-2-ylmethyl)benzylamine)$_2$]}[18]).

In tail-to-tail interactions of benzimidazole rings, the common parameters are depicted in Scheme 2(I), and they include the distance of center-to-center (a), the distance of center-to-face (b), the distance of the horizontal displacement (c), and the slippage angle (θ). These values for **2**, **3** and known complexes[15, 19] are given in Table 2. The values of **2** and **3** are fall in the normal ranges reported. The dihedral angles of two π systems in π-π interactions should be less than 20°,[20] and only so can π-π interactions occur effectively. Generally, the overlap of π systems adopts offset or displaced geometry. Therefore, there exist a slippage angle between two π systems, and a near or perfect face-to-face alignment of π systems is rare. The difference of parameters in the different

compounds may be related to the size and polarity of π systems, the metal atoms connected to heteroatoms, and the steric hindrance around π systems.

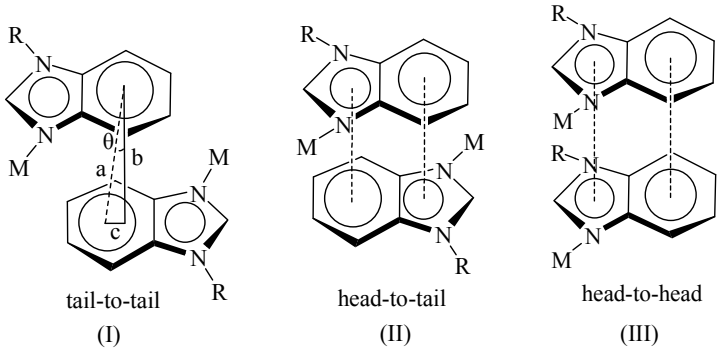

Scheme 2 π-π interactions of benzimidazole rings

Table 2 The parameters of π-π interactions between two π systems for **2**, **3** and known complexes

Complexes	a (Å)	b (Å)	c (Å)	θ (°)	dihedral angles (°)
2	3.775(4)	3.545(3)	1.296(1)	20.0(1)	5.0(1)
3	3.721(1)	3.427(1)	1.450(1)	22.9(1)	0.0(1)
Values of lit.[i]	3.0-7.0	3.3-3.8	1.0-3.0	17.0-40.0	< 20.0

[i] π systems from known complexes contain benzene, benzene with substituents or pyridine.

In the crystal packings of **4**, 1D polymeric chains are linked together through C-H···π contacts[13] to form 2D supramolecular layer (Fig. 4(b)). Additionally, 2D supramolecular layers are extended further into 3D supramolecular frameworks through C-H···π contacts (Fig. 4(c)). In C-H···π contacts, the hydrogen atoms are from CH_3 of DMF, and π systems are from benzimidazole rings (the data of C-H···π contacts being given in Table S1).

The conformations of dibenzimidazolyl bidentate ligand L and its metal complexes

According to literature reports and our results obtained, the dibenzimidazolyl bidentate ligand **L** with 2,3,5,6-tetramethylbenzene linker can rotate freely around -CH_2- groups, and it contains mainly two conformations when coordinating to the central metals (Scheme 3), namely, *cis*-conformations (such as in **I** and **II**) and *trans*-conformations (such as in **III-V**). In the *cis*-conformation, two benzimidazole rings lie in the same side of 2,3,5,6-tetramethylbenzene plane and point to the same direction. In the

trans-conformation, two benzimidazole rings lie in two sides of 2,3,5,6-tetramethylbenzene plane and point to the opposite directions.

The complexes based on ligand **L** contain mainly five types of conformations: (1) The metallomacrocycle (**I**) formed by two bidentate ligands and two metal atoms (such as $[Ag_2L_2](CF_3SO_3)_2$,[21, 22] $[Pd_2L_2Cl_4]\cdot 1.5CH_2Cl_2$[23] and $[Pd_2L_2Cl_4]\cdot 2CHCl_3$[23]); (2) The cage structure (**II**) formed by three bidentate ligands and two metal atoms (such as $[Ag_2L_3](CF_3SO_3)_2$[21, 22, 24]); (3) 1D polymeric chain (**III**) formed by the bidentate ligands and metal atoms, in which 1D polymeric chain adopts zig-zag coordination geometry (such as complexes **4-6**); (4) 2D network layer with triangular metallomacrocycle (**IV**), in which each metallomacrocycle monomer is constructed via three bidentate ligands and three metal atoms, and each metal center is surrounded by six benzimidazole rings (such as complex **1** and $\{[CoL_3](ClO_4)_2\}_n$[12(b)]); (5) 2D network layer with quadrangular metallomacrocycles (**V**), in which each metallomacrocycle monomer is constructed via four bidentate ligands, six metal atoms and four sulfate groups (like complex **2**). Additionally, when the bidentate ligand **L** and other compounds (like organic diacid) as mixed ligands are coordinated to metal atoms, 2D network layer with quadrangular metallomacrocycles (analogous to **V**) can also be afforded (like complex **3**). In short, when ligand **L** coordinates to the central metals, the *cis*-conformation ligand forms mainly complexes **I** and **II**, and the *trans*-conformation ligand forms mainly complexes **III-V**.

By comparison, the metal complexes from the dibenzimidazolyl bidentate ligands with flexible linkers (such as oligoether and alkanyl)[9] or semi-rigid linker (like -CH_2-2,3,5,6-tetramethylbenzene-CH_2-) contain some similar conformations, such as: (1) the metallomacrocycle formed by two ligands and two metal atoms, (2) 1D polymeric chain and (3) 2D network layer. But there also exist some differences in the conformations of metal complexes. The main difference is that the complexes from the ligand with semi-rigid linker (-CH_2-2,3,5,6-tetramethylbenzene-CH_2-) contain cage conformation,[21, 22, 24] and the complexes from the ligands with flexible linkers do not contain this type of conformation. The reason may be the structure of ligands with semi-rigid linkers is easier to fix than the structure of ligands with flexible linkers. This result affords a possible way for the preparation of cage complexes. Additionally, it is

worth noting that the dibenzimidazolyl bidentate ligands with oligoether linker more easily form the metallomacrocycle than the ligand with alkanyl linker due to the special structure of ether chain. Therefore, each type of conformation of metal complexes based on the ligands with oligoether linkers contains metallomacrocycle.[9a] On the whole, the conformations of metal complexes based on the dibenzimidazolyl bidentate ligands with flexible or semi-rigid linkers are related mainly to the conformation of ligands, difference of linkers, metal ions, counter-ions, the steric hindrance around metal centers, as well as the reaction conditions (such as solvent and the ratio of ligand and metal salt).

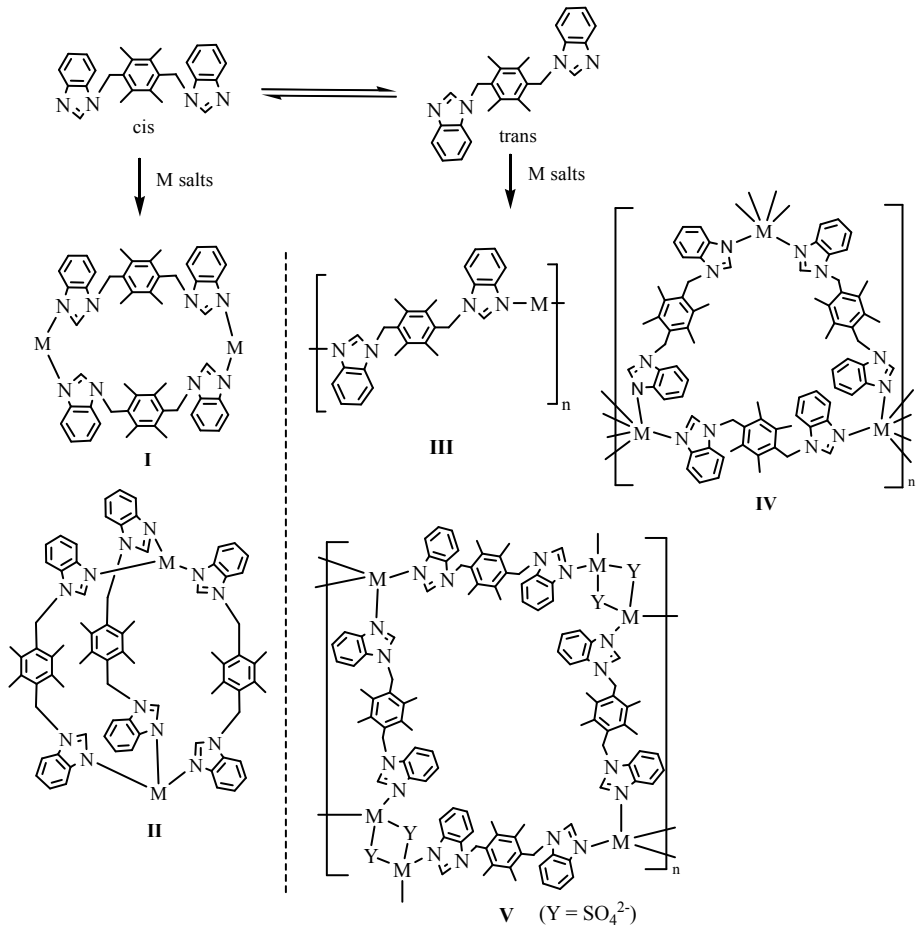

Scheme 3 The conformations of dibenzimidazolyl bidentate ligand **L** and its metal complexes

IR spectra analysis of 1-6

Complexes **1-6** have similar infrared spectra because their ligands are analogous. In each case, the absorption peaks around 1617-1610 cm^{-1} may result from υ(C=N) of imidazole

rings. The peaks in the region of 1235-1227 cm^{-1} originate from υ_s(C-C) and υ_s(C-N) of benzimidazole rings. The peaks in the region of 1663-1559 cm^{-1} may ascribed to the C-H bending vibrations. The absorption peaks around 3000-2800 cm^{-1} can be assigned to aromatic υ(C-H) modes. In complex **1**, the absorption peak at the 1110 cm^{-1} may be ascribed to the existence of perchlorate groups. In complex **2**, the absorption peak at the 1112 cm^{-1} and 615 cm^{-1} may be ascribed to the existence of sulfate groups, and the broad peak centered at 3416 cm^{-1} is attributed to the stretch vibrations of O-H from water molecule. The strong bands at 1653 cm^{-1} and 1571 cm^{-1} for **3** are observed, which are corresponding to the carbonyl groups and C=C in fumaric acid, and the broad peaks centered at 3464 cm^{-1} and 3411 cm^{-1} are attributed to the stretch vibrations of O-H from water molecule and methanol molecule. The absorption peaks at 1286 cm^{-1} for **4**, 1283 cm^{-1} for **5**, 1280 cm^{-1} for **6** may result from the existence of nitrate groups.

Fluorescence emission spectra of ligand L and complexes 1-6

As indicated in Fig. 5, the fluorescence emission spectra of ligand **L** and complexes **1-6** in acetonitrile at room temperature are obtained upon excitation at 245 nm. Ligand **L** shows triple emission bands at 310 nm, 330 nm and 415 nm, corresponding to intraligand transitions.[25] Complexes **1**, **2** and **5** exhibit also triple emission bands in the same regions (the fluorescence emission spectra of **3** and **4** are similar to that of **1**, and the fluorescence emission spectrum of **6** is similar to that of **5**), but they are stronger than that of ligand **L**, which should originate from the metal perturbed intraligand processes.[26] These complexes may have potential applications for fluorescent material.

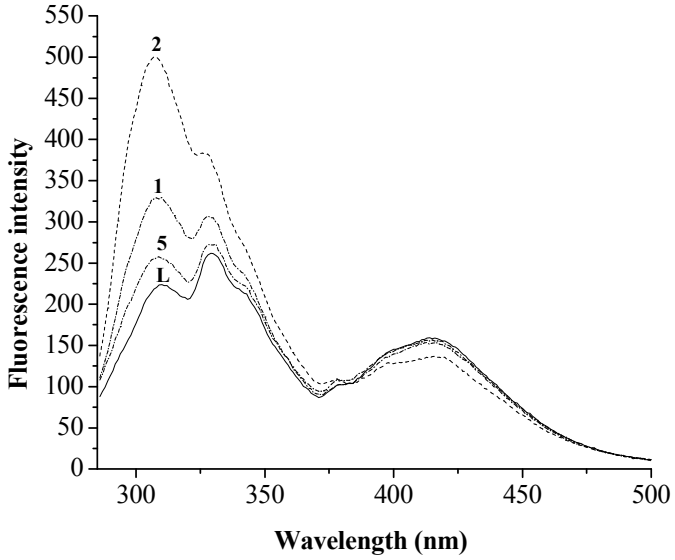

Fig. 5 Emission spectra of of ligand **L** and complexes **1**, **2** and **5** at 298 K in CH_3CN (5.0 × 10^{-5} M) solution.

Magnetic studies for complexes 2-4.

The variable-temperature magnetic susceptibilities for complexes **2-4** were measured on polycrystalline samples between 2 K to 300 K at 1000 Oe. The $\chi_m T$ value of **2** (0.69 cm^3 K/mol) at 300 K is slightly lower than the expected value ($\chi_m T$ = 0.75 cm^3 K/mol) for two isolated Cu^{2+} ions (S = 1/2 and g = 2.0) (Fig. 6). Upon cooling, the $\chi_m T$ value continuously decrease to reach a value of 0.18 cm^3 K/mol at 2 K, suggesting an antiferromagnetic coupling within binuclear Cu^{2+} units.

Considering the magnetic exchange interaction occurs between the Cu^{2+} ions within the SO_4^{2-} bridged dimer and between the two adjacent dimers across the hydrogen bonds, the best fits were obtained by using the binuclear model for S = 1/2 (equ. 1),[27] where J is the coupling constant within the dimer, ρ denotes the fraction of paramagnetic impurity in the sample , and the other symbols have the usual meanings.

$$\chi_M = \frac{2Ng^2\beta^2}{kT} \times \frac{1}{3 + e^{-2J/kT}} \times (1 - \rho) + \frac{Ng^2\beta^2}{2kT}\rho \quad \text{(equ. 1)}$$

The fitting of magnetic data over 100-300 K resulted to the parameters of g = 2.01, J = -24.2 cm^{-1}, ρ = 3.4% and R = 4.2 × 10^{-3}. The negative J value confirms the moderately

antiferromagnetic coupling within the Cu^{2+} dimer.

In Co(II) complexes **3** and **4** (Fig. 7 and Fig. 8), the $\chi_m T$ values are 2.90 cm^3 K/mol for **3** and 2.85 cm^3 K/mol for **4** at 300 K. These values are larger than the expected value ($\chi_m T$ = 1.87 cm^3 K/mol) for high spin Co^{2+} ions (S = 3/2 and g = 2.0) with octahedral coordination geometry and are in accordance with the well-documented orbital contribution of the octahedral Co^{2+} ions. Upon cooling, the $\chi_m T$ values continuously decrease to reach the values of 1.69 cm^3 K/mol for **3** and 1.50 cm^3 K/mol for **4** at 2 K due to the spin-orbital couplings of Co^{2+} ions and/or antiferromagnetic interactions between adjacent spin centers.

The magnetic data of **3** and **4** were analyzed by the Rueff's phenomenological model.[28] The best fitted values obtained are as follows: A + B = 3.13 cm^3 K mol^{-1}, E_1/k = 40.3 K, and E_2/k = 0.20 K for **3**, and A + B = 2.89 cm^3 K mol^{-1}, E_1/k = 28.7 K, and E_2/k = 0.21 K for **4**. Therefore, the magnetic coupling constant between Co^{2+} ions of **3** and **4** are -0.40 cm^{-1} and -0.42 cm^{-1}, respectively, based on the relationship of $\chi_M T \propto \exp(J/2kT)$. The small values of magnetic coupling are in accordance with the isolated Co^{2+} system. The decreases of $\chi_M T$ are mainly due to the contribution of spin-orbital coupling of Co^{2+} ion.

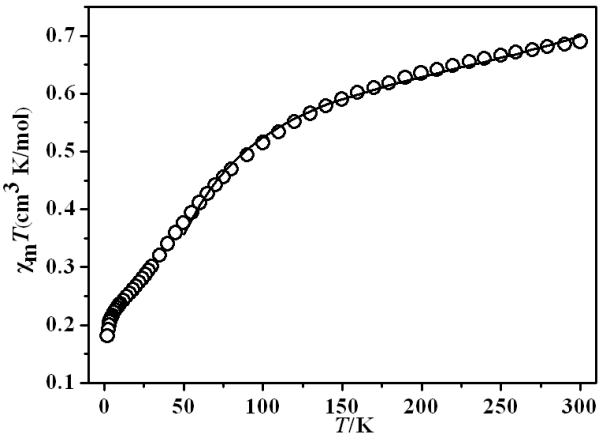

Fig. 6 The plot of $\chi_m T$ vs T for complex **2**. The solid line represents the best fit indicated in the text.

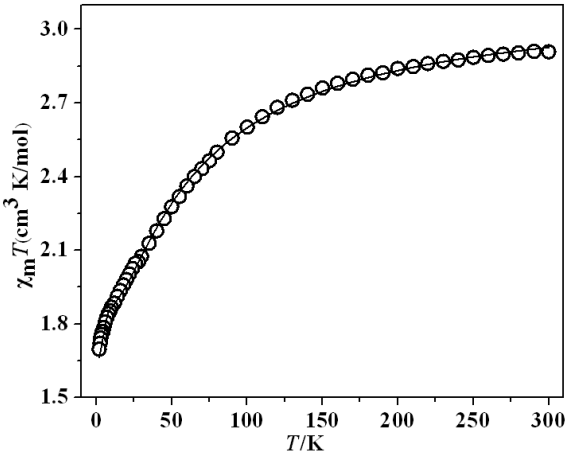

Fig. 7 The plot of $\chi_m T$ vs T for complex **3**. The solid line represents the best fit indicated in the text.

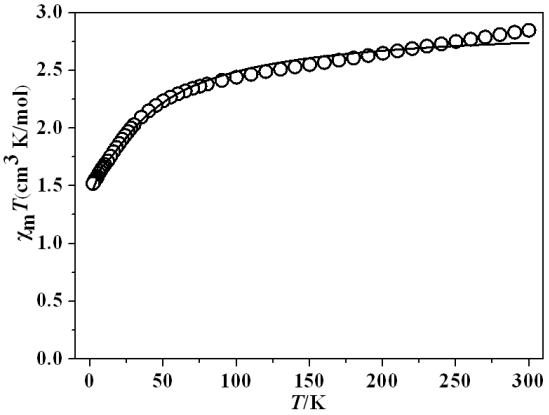

Fig. 8 The plot of $\chi_m T$ vs T for complex **4**. The solid line represents the best fit indicated in the text.

Powder X-ray diffraction of complexes 1-6

In order to establish their crystalline phase purity, powder X-ray diffraction (PXRD) experiments were carried out on complexes **1-6**. As shown in the PXRD patterns (Fig. S3-S8), the excellent agreement between the experimental PXRD patterns of the bulk samples **1-6** and the patterns simulated from the single-crystal data of **1-6** proved the crystalline phase purity of the corresponding complexes **1-6**.

Thermogravimetric analyses of complexes 1-6

To examine the thermal stability of **1-6**, the thermogravimetric analyses for crystal

samples of **1-6** were performed under a flowing nitrogen atmosphere with a heating rate of 20 ˚C min^{-1} from ambient temperature up to 800 ˚C. The TG curve of **1** indicates that this complex has high thermal stability (Fig. S9). It remains stable up to 282.2 ˚C, and experiences almost one-step weight loss of 60.81% from 282.2 ˚C to 396.2 ˚C, which is attributed to the thermal decomposition of the organic components, and does not stop until heating ends at 800 ˚C. Complex **2** starts to decompose from ambient temperature to 68.3 ˚C (Fig. S10), which reveals that the loss of 1.5 equiv. of free water molecules (calcd: 4.50%, found: 4.61%), and it decomposes from 68.3 ˚C to 219.9 ˚C to represent the loss of 2 equiv. of coordinated water molecules (calcd: 6.00%, found: 5.93%). Then **2** experiences weight loss of 50.93% from 219.9 ˚C to 538.9 ˚C, which is attributed to the thermal decomposition of the organic components, and does not stop decomposing until heating ends at 800 ˚C. Complex **3** starts to decompose from ambient temperature to 134.3 ˚C (Fig. S11), which reveals the loss of 2 equiv. of free methanol molecules and 2 equiv. of coordinated methanol molecules (calcd: 18.66%, found: 18.75%). Then **3** experiences weight loss of 41.00% from 134.3 ˚C to 450.1 ˚C, which is attributed to the thermal decomposition of the organic components, and does not stop decomposing until heating ends at 800 ˚C. Complexes **4-6** remain stable up to 166.3 ˚C for **4**, 160.4 ˚C for **5** and 179.1 ˚C for **6**, respectively (Fig. S12-S14). They experience weight losses of 11.36% (calcd: 11.23%) from 166.3 ˚C to 254.2 ˚C for **4**, 10.28% (calcd: 10.38%) from 155.3 ˚C to 241.1 ˚C for **5** and 11.01% (calcd: 11.15%) from 174.1 ˚C to 264.7 ˚C for **6**, which represent the loss of 1 equiv. of DMF, respectively. Then they experience the second weight losses of 29.94% from 285.4 ˚C to 298.2 ˚C for **4**, 20.65% from 325.8 ˚C to 378.2 ˚C for **5** and 21.13% from 320.6 ˚C to 374.6 ˚C for **6**, which are attributed to the thermal decomposition of the organic components, and do not stop decomposing until heating ends at 800 ˚C.

Conclusions

The six Mn(II), Co(II), Cu(II) and Cd(II) complexes have been prepared and characterized. In complex **1**, 2D layer with 39-membered rotiform metallomacrocycles is formed by ligand **L** and Mn(II) atoms, in which each rotiform metallomacrocycle is constructed by three bidentate ligands **L** and three Mn(II) atoms. In complex **2**, 2D layer

with 60-membered metallomacrocycles is formed via ligands **L**, Cu(II) atoms and SO_4^{2-}, in which each metallomacrocycle is constructed by four ligands **L**, six Cu(II) atoms and four sulfate groups. In complex **3**, ligand **L** along with fumarate groups participate in coordination with Co(II) atoms to form 2D layer with 44-membered metallomacrocycles, in which each metallomacrocycle is constructed by two bidentate ligands **L**, two fumarate groups and four Co(II) atoms. In complexes **4**-**6**, 1D polymeric chains are formed via ligand **L** and metal centers, in which 1D polymeric chains adopt zig-zag coordination geometry. In the crystal packings of complexes **1**-**6**, 2D supramolecular layers and 3D supramolecular frameworks are formed via intermolecular weak interactions, including π-π interactions and C-H···π contacts. In π-π interactions of two benzimidazole rings, the order of stability is: tail-to-tail > head-to-tail > head-to-head due to difference of arrangement. The dibenzimidazolyl bidentate ligand **L** with 2,3,5,6-tetramethylbenzene linker adopts two different conformations (*cis*- and *trans*-) when coordinating to the central metals, and its complexes contain mainly five types of conformations. The main difference of the dibenzimidazolyl bidentate ligands with semi-rigid linker (-CH_2-2,3,5,6-tetramethylbenzene-CH_2-) or flexible linkers (oligoether and alkanyl) when coordinating to the central metals is that the ligands with semi-rigid linker can form cage structure, but the ligands with flexible linker can not form this type of compound. Additionally, the metallomacrocyclic structures of these metal complexes suggest that they may have potential applications in the host-guest chemistry.

Experimental

General procedures

1,4-Bis(bromomethyl)-2,3,5,6-tetramethylbenzene[29] and 1,4-bis(benzimidazol-1-ylmethyl)-2,3,5,6-tetramethylbenzene[22] were prepared according to analogous methods reported. All the reagents for synthesis and analyses were of analytical grade and used without further purification. Melting points were determined with a Boetius Block apparatus. ^{1}H NMR spectra were recorded on a Varian Mercury Vx 400 spectrometer at 400 MHz. Chemical shifts, δ, were reported in ppm relative to the internal standard TMS for ^{1}H NMR, and J values were given in Hz. The elemental analyses of all compounds were obtained from the powder compounds recrystallised, and

measured using a Perkin-Elmer 2400C Elemental Analyzer. IR spectra (KBr) were taken on an Bruker Equinox 55 spectrometer. The luminescent spectra were conducted on Cary eclipse fluorescence spectrophotometer. The variable-temperature magnetic susceptibilities were performed on SQUID magnetometer. The powder X-ray diffracttion was recorded on aD/Max-IIIAdiffractometer with a Cu-target tube (λ = 1.5418 Å) and a graphite monochromator. Thermogravimetric analysis (TG) was performed in N_2 at a heating rate of 20 ˚C min on a NETZSCH TG209F3.

Preparation of 1,4-bis(benzimidazol-1-ylmethyl)-2,3,5,6-tetramethylbenzene (L). To a mixture of 2,3,5,6-tetramethylbenzene (13.420 g, 100.0 mmol), paraformaldehyde (6.150 g, 205.0 mmol) and glacial acetic acid (50 mL), was added rapidly a 31 wt% HBr/acetic acid solution (20 mL). The mixture was stirred for 8 h at 120 ˚C, and then poured into water (100 mL). The product was filtered and dried in vacuum. The 1,4-bis(bromomethyl)-2,3,5,6-tetramethylbenzene as a white powder was obtained. Yield: 31.050 g (97%). Mp: 192-194 ˚C.

A CH_3CN (100 mL) solution of benzimidazole (1.075 g, 9.1 mmol), KOH (1.000 g, 17.8 mmol), and tetrabutylammonium bromide (0.130 g, 0.4 mmol) was stirred for 1 h under refluxing, and then 1,4-bis(bromomethyl)-2,3,5,6-tetramethylbenzene (1.440 g, 4.5 mmol) was slowly added to above solution and stirred continually for 3 days at 80 ˚C. A pale yellow powder was obtained after removing the solvent. The powder was dissolved in CH_2Cl_2 (100 mL) and washed with water (3 × 100 mL), and the organic layer was dried over anhydrous $MgSO_4$. After removing CH_2Cl_2, a white powder of 1,4-bis(benzimidazol-1-ylmethyl)-2,3,5,6-tetramethylbenzene (**L**) was obtained. Yield: 1.543 g (88%). Mp: 238-240 ˚C. Anal. Calc. for $C_{26}H_{26}N_4$: C, 79.16; H, 6.64; N, 14.20%. Found: C, 79.33; H, 6.78; N, 14.43 %. ^{1}H NMR (400 MH_Z, DMSO-d_6): δ 2.21 (s, 12H, CH_3), 5.51 (s, 4H, CH_2), 7.22-7.31 (m, 4H, Ph*H*), 7.63 (d, J = 7.6 Hz, 2H, Ph*H*), 7.68 (d, J = 7.6 Hz, 2H, Ph*H*), 7.72 (s, 2H, 2-bim*H*). IR (KBr, cm^{-1}): 3047m, 2913m, 2363w, 1768w, 1610m, 1485s, 1384m, 1321m, 1283m, 1210vs, 1005m, 888m, 746vs (bim = benzimidazole).

Preparation of $\{[Mn(L)_3](ClO_4)_2\}_n$ (1). A N, N-dimethylformamide (DMF) solution (10 mL) containing **L** (0.100 g, 0.3 mmol) was added to a methanol solution (10 mL) of

$Mn(ClO_4)_2·6H_2O$ (0.217 g, 0.6 mmol). The mixture was stirred for 30 min at about 40 ˚C. The filtrate was allowed to evaporate slowly under ambient conditions, and colorless single crystals suitable for X-ray analysis were obtained within two weeks. Yield: 0.062 g (64%). Mp: > 320 ˚C. Anal. Calc. for $C_{78}H_{78}Cl_2MnN_{12}O_8$: C, 65.17; H, 5.46; N, 11.69%. Found: C, 65.33; H, 5.57; N, 11.53%. IR (KBr, cm^{-1}): 3447vs, 2958w, 2361w, 1651m, 1612m, 1559m, 1508m, 1458m, 1406w, 1312w, 1229m, 1187w, 1110m, 903m, 748m, 621m.

Preparation of $[Cu(L)(SO_4)(H_2O)]·1.5H_2O$ (2). This complex was prepared in a manner analogous to that of **1**, and only instead of $Mn(ClO_4)_2·6H_2O$ with $CuSO_4·5H_2O$ (0.150 g, 0.6 mmol), and blue single crystals suitable for X-ray analysis were obtained within two weeks. Yield: 0.050 g (59%). Mp: 292-294 ˚C. Anal. Calc. for $C_{26}H_{31}CuN_4O_{6.5}S$: C, 52.12; H, 5.21; N, 9.35%. Found: C, 52.54; H, 5.14; N, 9.62%. IR (KBr, cm^{-1}): 3461vs, 3416vs, 2964w, 2913w, 1634s, 1615m, 1568m, 1413w, 1337w, 1232w, 1163w, 1112m, 1061w, 1030w, 745m, 665m, 615m.

Preparation of $[Co(L)(L_A)(CH_3OH)_2]·2CH_3OH$ (3). A DMF solution (10 mL) containing fumaric acid (0.100 g, 0.3 mmol) was added to a methanol solution (10 mL) of **L** (0.100 g, 0.3 mmol). After *ca*. 3 min of vigorous mixing, an aqueous solution (5 mL) of $Co(NO_3)_2·6H_2O$ (0.175 g, 0.6 mmol) was added and the pH value of the solution was adjusted to approximated 7 by triethylamine. The mixture was continually stirred for 30 min at about 40 ˚C. The filtrate of the mixture was allowed to evaporate slowly under ambient conditions, and purple single crystals suitable for X-ray analysis were obtained within two weeks. Yield: 0.085 g (63%). Mp: > 320 ˚C. Anal. Calc. for $C_{34}H_{44}CoN_4O_8$: C, 58.70; H, 6.37; N, 8.05%. Found: C, 59.13; H, 6.12; N, 8.24%. IR (KBr, cm^{-1}): 3464vs, 3411vs, 2958m, 2923m, 2363w, 1653s, 1637s, 1616s, 1571vs, 1384vs, 1292m, 1229m, 1007w, 973w, 912w, 840w, 745m, 678m.

Preparation of $[Co(L)(DMF)(NO_3)_2]_n$ (4). This complex was prepared in a manner analogous to that of **1**, and only instead of $Mn(ClO_4)_2·6H_2O$ with $Co(NO_3)_2·6H_2O$ (0.175 g, 0.6 mmol), and purple single crystals suitable for X-ray analysis were obtained within two weeks. Yield: 0.051 g (60%). Mp: > 320 ˚C.. Anal. Calc. for $C_{29}H_{33}CoN_7O_7$: C, 53.54; H, 5.11; N, 15.07%. Found: C, 53.42; H, 5.41; N, 15.32%. IR (KBr, cm^{-1}): 3445m, 2945w, 1698m, 1660vs, 1612m, 1524m, 1467vs, 1381vs, 1311s, 1286s, 1229m, 1194m,

1115w, 1033w, 916w, 871w, 833w, 814w, 760m, 751m, 688m.

Preparation of $[Cd(L)(DMF)(NO_3)_2]_n$ (5). This complex was prepared in a manner analogous to that of **1**, and only instead of $Mn(ClO_4)_2 \cdot 6H_2O$ with $Cd(NO_3)_2 \cdot 4H_2O$ (0.185 g, 0.6 mmol), and colorless single crystals suitable for X-ray analysis were obtained within two weeks. Yield: 0.062 g (58%). Mp: > 320 ˚C. Anal. Calc. for $C_{29}H_{33}CdN_7O_7$: C, 49.47; H, 4.72; N, 13.92%. Found: C, 49.41; H, 4.68; N, 13.98%. IR (KBr, cm^{-1}): 3550s, 3477vs, 3420vs, 2939w, 2910w, 2356w, 1666s, 1631s, 1612s, 1520m, 1441m, 1381m, 1302m, 1283m, 1229m, 1188w, 1115w, 1033w, 909w, 817w, 757m, 745w.

Preparation of $[Cu(L)(DMF)(NO_3)_2]_n$ (6). This complex was prepared in a manner analogous to that of **1**, and only instead of $Mn(ClO_4)_2 \cdot 6H_2O$ with $Cu(NO_3)_2 \cdot 3H_2O$ (0.177 g, 0.6 mmol), and blue single crystals suitable for X-ray analysis were obtained within two weeks. Yield: 0.051 g (60%). Mp: 258-260 ˚C. Anal. Calc. for $C_{29}H_{33}CuN_7O_7$: C, 53.16; H, 5.07; N, 14.96%. Found: C, 53.45; H, 5.38; N, 14.76%. IR (KBr, cm^{-1}): 3464vs, 3417vs, 2932w, 2356w, 1660s, 1615m, 1527s, 1460s, 1381s, 1299vs, 1280s, 1229s, 1178m, 1112w, 1023m, 925m, 843w, 811w, 760s, 745s, 675m.

X-ray data collection and structure determinations. X-ray single-crystal diffraction data for complexes **1** and **3**-**6** were collected by using a Bruker Apex II CCD diffractometer at 173(2) K (complex **2** at 296(2) K) with Mo-Ka radiation (λ = 0.71073 M) by ω scan mode. There was no evidence of crystal decay during data collection in all cases. Semiempirical absorption corrections were applied by using SADABS and the program SAINT was used for integration of the diffraction profiles.[30] All structures were solved by direct methods by using the SHELXS program of the SHELXTL package and refined with SHELXL[31] by the full-matrix least-squares methods with anisotropic thermal parameters for all non-hydrogen atoms on F^2. Hydrogen atoms bonded to C atoms were placed geometrically and presumably solvent H atoms were first located in difference Fourier maps and then fixed in the calculated sites. The hydrogen atoms of water molecules for complex **2** or methanol molecules for complex **3** could not be located and calculated due to the disorder of the parent atoms.[28(c)] Further details for crystallographic data and structural analysis are listed in Table **3** and Table **4**, which were generated by using Crystal-Maker.[32] The data of bond distances and angles for **1**-**6** are given in Table S3 of Supplementary Information.

Table 3 Crystal data and structure refinements for **1-3**

	1	**2**	**3**
chemical formula	$C_{78}H_{78}Cl_2MnN_{12}O_8$	$C_{26}H_{28}CuN_4O_5S \cdot 1.5H_2O$	$C_{32}H_{36}CoN_4O_6 \cdot 2CH_3OH$
fw	1437.36	599.15	695.66
Cryst syst	Trigonal	Monoclinic	Triclinic
space group	*P*-3	$P2_1/c$	$P\bar{1}$
a /Å	13.468(1)	12.608(2)	9.144(4)
b /Å	13.468(1)	13.831(3)	9.914(4)
c /Å	10.496(1)	17.334(2)	10.981(5)
α /deg	90	90	113.2(6)
β /deg	90	119.5(9)	104.0(7)
γ /deg	120	90	92.3(7)
V /Å^3	1649.0(3)	2628.9(8)	876.8(7)
Z	1	4	1
D_{calcd}, Mg/m^3	1.447	1.537	1.317
Abs coeff, mm^{-1}	0.353	0.964	0.544
F(000)	753	1268	367
Cryst size, mm	0.13 × 0.10 × 0.08	0.17 × 0.15 × 0.14	0.15 × 0.14 × 0.13
θ_{min}, θ_{max}, deg	1.75, 25.00	1.86, 25.01	2.26, 25.01
T /K	173(2)	296(2)	173(2)
no. of data collected	8453	13201	4469
no. of unique data	1953	4632	3069
no. of refined params	155	356	228
goodness-of-fit on F^2 [a]	1.025	1.028	1.059
Final *R* indices[b] $[I > 2\sigma(I)]$			
R_1	0.0478	0.0515	0.0608
wR_2	0.0919	0.1208	0.1625
R indices (all data)			
R_1	0.0791	0.0776	0.0739
wR_2	0.1039	0.1366	0.1734

[a] Goof = $[\Sigma\omega(F_o^2 - F_c^2)^2 /(n-p)]^{1/2}$, where *n* is the number of reflection and *p* is the number of parameters refined. [b] R1 = $\Sigma(||F_o| - |F_c||)/\Sigma|F_o|$; wR2 = $1/[\sigma^2(F_o^2) + (0.0691P) + 1.4100P]$ where $P = (F_o^2 + 2F_c^2)/3$.

Table 4 Crystal data and structure refinements for **4-6**

	4	**5**	**6**
chemical formula	$C_{29}H_{33}CoN_7O_7$	$C_{29}H_{33}CdN_7O_7$	$C_{29}H_{33}CuN_7O_7$
fw	650.55	704.02	655.16
Cryst syst	Monoclinic	Monoclinic	Monoclinic
space group	*C*2/*c*	*C*2/*c*	*C*2/*c*
a /Å	16.620(3)	16.651(5)	16.271(3)
b /Å	9.529(1)	9.660(3)	9.664(3)
c /Å	19.384(4)	19.921(7)	19.485(5)
α /deg	90	90	90
β /deg	104.2(5)	105.8(5)	103.8(6)
γ /deg	90	90	90
V /Å^3	2975.7(1)	2628.9(8)	2975.4(1)
Z	4	4	4
D_{calcd}, Mg/m^3	1.452	1.517	1.463
Abs coeff, mm^{-1}	0.636	0.766	0.793
F(000)	1356	1440	1364
Cryst size, mm	0.17 × 0.16 × 0.15	0.15 × 0.14 × 0.13	0.15 × 0.14 × 0.13
θ_{min}, θ_{max}, deg	2.17, 25.01	2.13, 25.01	2.15, 25.00
T /K	173(2)	173(2)	173(2)
no. of data collected	7248	7444	7307
no. of unique data	2626	2721	2630
no. of refined params	226	226	226
goodness-of-fit on F^2 [a]	1.027	1.006	1.061
Final *R* indices[b] [$I > 2\sigma(I)$]			
R_1	0.0715	0.0353	0.0512
wR_2	0.2381	0.0737	0.1230
R indices (all data)			
R_1	0.0857	0.0441	0.0777
wR_2	0.2543	0.0774	0.1367

[a] Goof = $[\Sigma\omega(F_o^2 - F_c^2)^2/(n-p)]^{1/2}$, where *n* is the number of reflection and *p* is the number of parameters refined. [b] R1 = $\Sigma(||F_o| - |F_c||)/\Sigma|F_o|$; wR2 = $1/[\sigma^2(F_o^2) + (0.0691P) + 1.4100P]$ where $P = (F_o^2 + 2F_c^2)/3$.

Acknowledgments

This work was financially supported by the National Natural Science Foundation of

China (No.21172172), Tianjin Natural Science Foundation (No.11JCZDJC22000) and the Program for Innovative Research Team in University of Tianjin (TD12-5038).

References

1 (*a*) J. M. Lehn, *Supramolecular Chemistry: Concepts and Perspectives*, VCH, Weinheim, 1995; (*b*) M. M. Conn and J. Jr. Rebek, *Chem. Rev.*, 1997, **97**, 1647-1668; (*c*) M. Fujita, J. Yazaki and K. Ogura, *J. Am. Chem. Soc*., 1990, **112**, 5645-5647; (*d*) R. M. Yeh, A. V. Davis and K. N. Raymond, *Supramolecular systems: self-assembly, in Comprehensive Coordination Chemistry II,* Elsevier Ltd., 2003, **7**, 327-355; (*e*) C. A. Schalley, A. Lözen and M. Albrecht, *Chem. Eur. J*., 2004, **10**, 1072-1080; (*f*) F. Würthner, C. C. Youand and C. R. Saha-Möller, *Chem. Soc. Rev*., 2004, **33**, 133-146; (*g*) A. Kumar, S. S. Sun and A. J. Lees, *Coord. Chem. Rev*., 2008, **252**, 922-939; (*h*) G. F. Swiegers and T. J. Malefetse, *Coord. Chem. Rev*., 2002, **225**, 91-121; (*i*) D. Fiedler, D. H. Leung, B. G. Bergman and K. N. Raymond, *Acc. Chem. Res*., 2005, **38**, 349-358; (*j*) M. Yoshizawa, J. K. Klosterman and M. Fujita, *Angew. Chem., Int. Ed*., 2009, **48**, 3418-3438; (*k*) D. R. Turner, A. Pastor, M. Alajarin and J. W. Steed, *Struct. Bonding*, 2004, **108**, 97-168.

2 (*a*) A. J. Blake, N. R. Champness, P. Hubberstey, W. S. Li, M. A. Withersby and M. Schröder, *Coord. Chem. Rev*., 1999, **183**, 117-138; (*b*) L. Carlucci, G. Ciani, P. Macchi and D. M. Proserpio, *Chem. Commun*., 1998, 1837.

3 (*a*) D. Whang and K. Kim, *J. Am. Chem. Soc*., 1997, **119**, 451-452; (*b*) D. P. Funeriu, J. M. Lehn, K. M. Fromm and D. Fenske, *Chem. Eur. J*., 2000, **6**, 2103-2111.

4 (*a*) L. R. MacGillivray and J. L. Atwood, *Angew. Chem. Int. Ed.*, 1999, **38**, 1018-1033; (*b*) B. H. Ye, M. L. Tong and X. M. Chen, *Coord. Chem. Rev.*, 2005, **249**, 545-565; (*c*) A. N. Khlobystov, A. J. Blake, N. R. Champness, D. A. Le menovskii, A. G. Majouga, N. V. Zyk and M. Schroder, *Coord. Chem. Rev.*, 2001, **222**, 155-192; (*d*) C. Janiak, *Dalton Trans.*, 2003, 2781-2804; (*e*) D. F. Sun, D. J. Collins, Y. X. Ke, J. L. Zuo and H. C. Zhou, *Chem. Eur. J.*, 2006, **12**, 3768-3776.

5 (*a*) S. Muthu, J. H. K. Yip and J. J. Vittal, *Dalton Trans*., 2002, 4561-4568; (*b*) T. L. Hennigar, D. C. MacQuarrie, P. Loiser, R. D. Rogers and M. J. Zaworotko, *Angew. Chem. Int. Ed. Engl.*, 1997, **36**, 972-973; (*c*) M. L. Tong, Y. M. Wu, J. Ru, X. M.

Chen, H. C. Chang and S. Kitagawa, *Inorg. Chem*., 2002, **41**, 4846-4848; (*d*) J. P. Zhang, X. C. Huang and X. M. Chen, *Chem. Soc. Rev*., 2009, **38**, 2385-2396.

6 (*a*) D. E. Wang, K. J. Deng, K. L. Lv and C. G. Wang, *CrystEngComm*, 2009, **11**, 1442-1450; (*b*) N. W. Ockwig, O. Delgado-Friedrichs, M. O´Keeffe and O. M. Yaghi, *Acc. Chem. Res*., 2005, **38**, 176-182; (*c*) K. N. Power, T. L. Hennigar and M. J. Zaworotko, *Chem. Commun*., 1998, 595; (*d*) N. L. Rosi, J. Kim, M. Eddaoudi, B. Chen, M. O´Keeffe and O. M. Yaghi, *J. Am. Chem. Soc*., 2005, **127**, 1504-1518; (*e*) L. K. Li, Y. L. Song, H. W. Hou, Y. T. Fan and Y. Zhu, *Eur. J. Inorg. Chem*., 2005, **16**, 3238-3249; (*f*) J. F. Ma, J. F. Liu, Y. C. Liu, Y. Xing, H. Q. Jia and Y. H. Lin, *New J. Chem*., 2000, **24**, 759-763; (*g*) C. H. Zhou, X. R. Gu, R. G. Xie and M. S. Cai, *Synth. Commun*., 1999, **29**, 1217-1222; (*h*) Y. L. Zhou, F. Y. Meng, J. Zhang, M. H. Zeng and H. Liang, *Cryst. Growth Des*., 2009, **9**, 1402-1410.

7 (*a*) R. J. Sundberg and R. B. Martin, *Chem. Rev*., 1974, **74**, 471-517; (*b*) K. Kurdziel and T. Glowiak, *Polyhedron*, 2000, **19**, 2183-2188.

8 (*a*) H. Jin, Y. F. Qi, E. B. Wang, Y. G. Li, X. L. Wang, C. Qin and S. Chang, *Cryst. Growth Des*., 2006, **6**, 2693-2698; (*b*) X. J. Li, R. Cao, D. F. Sun, W. H. Bi, Y. Q. Wang, X. Li and M. C. Hong, *Cryst. Growth Des*., 2004, **4**, 775-780; (*c*) M. Xue, G. S. Zhu, H. Ding, L. Wu, X. J. Zhao, Z. Jin and S. L. Qiu, *Cryst. Growth Des*., 2009, **9**, 1481-1488.

9 (*a*) Q. X. Liu, Z. X. Zhao, X. J. Zhao, Z. Q. Yao, S. J. Li and X. G. Wang, *Cryst. Growth Des*., 2011, **11**, 4933-4942; (*b*) Q. X. Liu, Q. Wei, X. J. Zhao, H. Wang, S. J. Li and X. G. Wang, *Dalton Trans.*, 2013, **42**, 5902-5915.

10 (*a*) M. Yuan, F. Zhao, W. Zhang, Z. M. Wang and S. Gao, *Inorg. Chem.*, 2007, **46**, 11235-11242; (*b*) B. J. Michael, J. W. Kampf, K. L. Martin and P. L. Vincent, *Inorg. Chem.*, 1995, **34**, 5252-5260; (*c*) K. S. Dube and T. C. Harrop, *Dalton trans.*, 2011, **40**, 7496-7498.

11 (*a*) S. Youngme, T. Chotkhun, N. Chaichit, G. A. van Albada and J. Reedijk, *Inorg. Chem. Comm.*, 2007, **10**, 843-848; (*b*) K. X. Huang, Z. J. Xu, Y. Z. Li and H. G. Zheng, *Cryst. Growth Des*., 2007, **7**, 202-204; (*c*) A. K. Paul, U. Sanyal and S. Natarajan, *Cryst. Growth Des*., 2010, **10**, 4161-4175; (*d*) D. Krishna Kumar, A. Das and P. Dastidar, *Cryst. Growth Des*., 2007, **7**, 205-207.

12 (*a*) Y. Gao, B. Twamley and J. M. Shreeve, *Inorg. Chem.*, 2006, **45**, 1150-1155; (*b*) C. Y. Su, Y. P. Cai, C. L. Chen and B. S. Kang, *Inorg. Chem.*, 2001, **40**, 2210-2211; (*c*) Y. M. Li, C. Y. Xiao, X. D. Zhang, Y. Q. Xu, H. J. Lun and J. Y. Niu, *CrystEngComm*, 2013, **15**, 7756-7762.

13 (*a*) G. R. Desiraju and T. Steiner, *The Weak Hydrogen Bond in Structural Chemistry and Biology*, Oxford University Press, Oxford, UK, 1999; (*b*) R. T. E. Tiekink and J. Zukerman-Schpector, *The Importance of Pi-Interactions in Crystal Engineering: Frontiers in Crystal Engineering*, First Edition. Published 2012 by John Wiley & Sons, Ltd; (*c*) A. L. Pickering, G. Seeber, D. L. Long and L. Cronin, *CrystEngComm*, 2005, **7**, 504-510; (*d*) R. P. A. Bettens, D. Dakternieks, A. Duthie, F. S. Kuan and E. R. T. Tiekink, *CrystEngComm*, 2009, **11**, 1362-1372.

14 (*a*) D. Venkataraman, S. Lee and J. S. Moore, *Nature*, 1994, **371**, 591-593; (*b*) M. Nishio, *CrystEngComm*, 2004, **6**, 130-158; (*c*) F. Klärner and B. Kahlert, *Acc. Chem. Res*., 2003, **36**, 919-932.

15 C. Janiak, *J. Chem. Soc., Dalton Trans*., 2000, 3885-3896.

16 (*a*) H. Y. Liu, J. F. Ma, Y. Y. Liua and J. Yang, *CrystEngComm*, 2013, **15**, 2699-2708; (*b*) J. L. Du, T. L. Hu, S. M. Zhang, Y. F. Zeng and X. H. Bu, *CrystEngComm*, 2008, **10**, 1866-1874; (*c*) X. P. Yang, R. A. Jones, M. M. Oye, M. Wiester and R. J. Lai, *New J. Chem*., 2011, **35**, 310-318; (*d*) X. L. Wang, J. Li, A. X. Tian, H. Y. Lin, G. C. Liu and H. L. Hu, *Inorg. Chem. Commun*., 2011, **14**, 103-106.

17 (*a*) Z. Q. Xia, Q. Wei, Q. Yang, C. F. Qiao, S. P. Chen, G. Xie, G. C. Zhang, C. S. Zhou and S. L. Gao, *CrystEngComm*, 2013, **15**, 86-99; (*b*) R. K. Pathak, V. K. Hinge, P. Mondal and C. P. Rao, *Dalton Trans*., 2012, **41**, 10652-10660; (*c*) X. J. Hong, M. F. Wang, H. G. Jin, Q. G. Zhan, Y. T. Liu, H. Y. Jia, X. Liua and Y. P. Cai, *CrystEngComm*, 2013, **15,** 5606-5611; (*d*) A. Jabłońska-Wawrzycka, P. Rogala, S. Michałkiewicz, M. Hodorowiczb and B. Barszcza, *Dalton Trans*., 2013, **42**, 6092-6101; (*e*) K. M. Lee, C. K. Lee and I. J. B. Lin, *CrystEngComm*, 2010, **12,** 4347-4351.

18 H. L. Wu, J. K. Yuan, Y. Bai, G. L. Pan, H. Wang, J. Kong, X. Y. Fan and H. M. Liu, *Dalton Trans*., 2012, **41**, 8829-8838.

19 (*a*) Y. S. Chong, W. R. Carroll, W. G. Burns, M. D. Smith and K. D. Shimizu, *Chem. Eur. J*., 2009, **15**, 9117-9126; (*b*) S. E. Snyder, B. S. Huang, Y. W. Chu, H. S. Lin and J.

R. Carey, *Chem. Eur. J*., 2012, **18**, 12663-12671.

20 S. E. Snyder, B. S. Huang, Y. W. Chu, H. S. Lin and J. R. Carey, *Chem. Eur. J.*, 2012, **18**, 12663-12671.

21 (*a*) Q. Zhang, J. Y. Zhang, Q. Y. Yu, M. Pan and C. Y. Su, *Cryst. Growth Des*., 2010, **10**, 4076-4084; (*b*) C. L. Chen, J. Y. Zhang and C. Y. Su, *Eur. J. Inorg. Chem.,* 2007, 2997-3010.

22 C. Y. Su, Y. P. Cai, C. L. Chen, M. D. Smith, W. Kaim and H. C. Z. Loye , *J. Am. Chem. Soc.*, 2003, **125**, 8595-8613.

23 Q. Zhang, L. He, J. M. Liu, W. Wang, J. Y. Zhang and C. Y. Su, *Dalton Trans.*, 2010, **39**, 11171-11179.

24 C. Y. Su, Y. P. Cai, C. L. Chen, H. X. Zhang and B. S. Kang, *J. Chem. Soc*., *Dalton Trans*., 2001, 359-361.

25 (*a*) F. J. B. dit Dominique, H. Gornitzka, A. Sournia-Saquet and C. Hemmert, *Dalton Trans*., 2009, **38**, 340-352; (*b*) V. J. Catalano and A. L. Moore, *Inorg. Chem*., 2005, **44**, 6558-6566; (*c*) B. Liu, W. Chen and S. Jin, *Organometallics*, 2007, **26**, 3660-3667.

26 (*a*) S. C. Chan, M. C. W. Chan, Y. Wang, C. M. Che, K. K. Cheung and N. Zhu, *Chem. Eur. J*., 2001, **7**, 4180-4189; (*b*) V. W. W. Yam, K. L. Yu, K. M. C. Wong and K. K. Cheung, *Organometallics*, 2001, **20**, 721-726.

27 (*a*) Y. Song, D. R. Zhu, K. L. Zhang, Y. Xu, C.Y. Duan and X. Z. You, *Polyhedron*, 2000, **19**, 1461-1464; (*b*) X. Z. Wang, D. R. Zhu, Y. Xu, J. Yang, X. Shen, J. Zhou, N. Fei, X. K. Ke and L. M. Peng, *Cryst. Gorwth Des.*, 2010, **10**, 887-894.

28 (*a*) J. M. Rueff, C. Paulsen, J. Souletie, M. Drillon and P. Rabu, *Solid State Sci.*, 2005, **7**, 431-436; (*b*) F. S. Delgado, M. Hernández-Molina, J. Sanchiz, C. Ruiz-Pérez, Y. Rodríguez-Martín, T. López, F. Lloret and M. Julve, *CrystEngComm*, 2004, **6**, 106-111; (*c*) T. Gao, X. Z. Wang, H. X. Gu, Y. Xu, X. Shen and D. R. Zhu, *CrystEngComm*, 2012, **14**, 5905-5913; (*d*) E. C. Yang, Y. Feng, Z. Y. Liu, T. Y. Liu and X. J. Zhao, *CrystEngComm*, 2011, **13**, 230-242.

29 A. W. van der Made and R. H. van der Made, *J. Org. Chem*., 1993, **58**, 1262-1263.

30 Bruker AXS, *SAINT Software Reference Manual*, Madison, WI, 1998.

31 Sheldrick, G. M. SHELXTL NT (Version 5.1), *Program for Solution and Refinement*

32 Palmer, D. C. Crystal Maker 7.1.5, *CrystalMaker Software*, Yarnton, UK, 2006.

A table of contents entry:

Six manganese(II), cobalt(II), copper(II) and cadmium(II) complexes based on dibenzimidazolyl ligands with 1,2,4,5-tetramethylbenzene linker have been prepared and characterized.

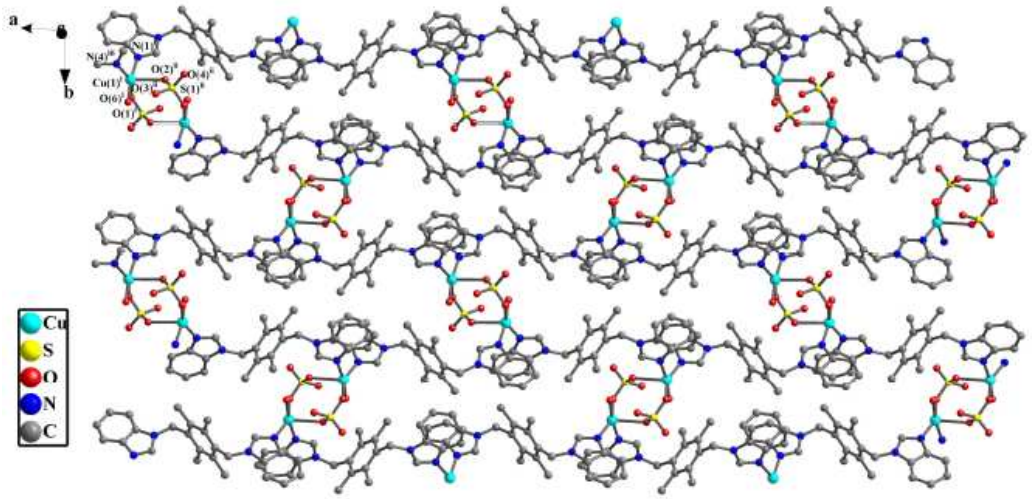

Software of Graphics:

L, $\mathbf{H_2L_A}$ and Schemes 1-3 : Chem Draw 8.0

Figures 1-4: Diamand 3.0

Figures 5-8: Origin 6.0